EUROGRAPHICS Workshop on Graphics and Cultural Heritage (2017)
T. Schreck and T. Weyrich (Editors)

Exploiting Unbroken Surface Congruity for the Acceleration of Fragment Reassembly

M.A. Savelonas[1], A. Andreadis[1], G. Papaioannou[1], P. Mavridis[2]

[1]Athens University of Economics and Business, Greece
[2]Graz University of Technology, Austria

Abstract

Virtual reassembly problems are often encountered in the cultural heritage domain. The reassembly or "puzzling" problem is typically described as the process for the identification of corresponding pieces within a part collection, followed by the clustering and pose estimation of multiple parts that result in a virtual representation of assembled objects. This work addresses this problem with an efficient, user-guided computational approach. The proposed approach augments the typical reassembly pipeline with a smart culling step, where geometrically incompatible fragment combinations can be quickly rejected. After splitting each fragment into potentially fractured and intact facets, each intact facet is examined for prominent linear or curved structures and a heuristic test is employed to evaluate the plausibility of facet pairs, by comparing the number of feature curves associated with each facet, as well as the geometric texture of associated intact surfaces. This test excludes many pairwise combinations from the remaining part of the reassembly process, significantly reducing overall time cost. For all facet pairs that pass the initial plausibility test, pairwise registration driven by enhanced simulated annealing is applied, followed by multi-part registration. The proposed reassembly approach is evaluated on real scanned data and our experiments demonstrate an increase in efficiency that ranges from 30% to more than 500% in some cases, depending on the number of culled combinations.

CCS Concepts

•***Computing methodologies*** → ***Shape analysis;*** •***Applied computing*** → ***Arts and humanities;***

1. Introduction

Reassembly of 3D objects from physical parts or fragments, from digital or digitized parts available in reference repositories, or from mixed sets of physical and digital fragments, is an instrumental task in the cultural heritage (CH) domain. Still, when performed manually, this task remains rather challenging and time consuming. Although an archaeologist is capable to identify complementary parts and associations in small collections of objects, this can quickly become impractical for large collections. More so, taking into account that fragments may be eroded or incomplete and dispersed in separate physical or digital collections. The digital counterpart, virtual object reassembly, has received significant research interest in the past years, mainly with regard to specialized object types, such as frescos and pottery. Beyond CH, virtual reassembly is applicable to the domains of forensics, mechanical engineering and computer-assisted surgery.

In the general case, the number of fragment combinations that should be tested by a virtual reassembly algorithm is exponential and the problem is known to be NP-hard [DD07], as is the case with similar 2D and 3D puzzle problems with uncertain fragment compatibility. Typically, computational reassembly starts with the digitization of physical fragments and continues with the preprocessing of fragment geometry in order to extract the fractured and intact surfaces or identify geometric priors that can produce associations between individual parts. All pairwise combinations of fragments are tested for alignment and a matching score is computed. This step usually begins with a *global registration* process that examines the solution search space for a good but rough alignment, which in turn initiates a *local registration* process in order to refine the solution. The complete set of pairwise results drives subsequently the multi-part registration, where complete objects are formed by finding the global position for each fragment.

Even from the very first attempts to address the virtual reassembly problem, it quickly became necessary to devise mechanisms for the pruning of the vast search space in both the pairwise registration and the multi-part assembly stages. One way to achieve this is by either lowering the dimensionality of the problem using application-specific priors, such as symmetry or shape planarity. For the general 2D and 3D case, many methods employ fast-to-compute heuristics to cull solutions early on that are likely to correspond to incompatible pairings (e.g. [PK03] and [FSTF*11]) or clusters of fragments (see for instance [SF16]).

DOI: 10.2312/gch.20171305

In this work, following the feature-curve-based reassembly framework of Andreadis et al. [APM15] and the reassembly system proposed in [PSA*17], we introduce a heuristic approach for limiting the pairwise combinations to be evaluated for alignment that exploits the additional information that can be extracted in this pipeline: we compare the number of *feature curves* associated with each potentially fractured facet, as well as the geometric texture of the adjacent intact surfaces. This test excludes many pairwise combinations from the remaining part of the reassembly process, significantly reducing the overall processing time. The facet combinations that are retained go through pairwise registration, which takes into account fractured surface shape and prominent curved or linear structures on the intact faces. In case of multiple fragments, assemblies are formed, followed by multi-part registration for the final adjustment of the pieces.

The rest of this paper is organized as follows: in Section 3 we provide an overview of related work in 3D object reassembly, in Section 3 we describe the proposed 3D object reassembly methodology, with emphasis on the novel heuristic. In Section 4 we present results of our approach, when applied to real scanned CH and contemporary objects. Finally, Section 5 provides the main conclusions derived from this study.

2. Related Work

It is important to note that Demaine and Demaine [DD07] have proved that the problem of jigsaw puzzles, and therefore the more general problem of 3D object reassembly, is NP-Hard. Therefore, all the methods in the literature use heuristic algorithms or approximations, in order to reach a solution within reasonable execution time.

Scheuering et al. [SRE*01] expect manual coarse positioning and utilize a voxel-based metric for optimal alignment. Willis et al. [WAT*07] and Zhou et al. [ZWS*09] initially segment the surfaces to intact and fractured ones, using density analysis and expect user interaction for the selection of fractured patches that coarsely correspond.

Another class of methods employ ICP variants. The method of Mellado et al. [MRS10] requires user-specified initial position and orientation and validates the pose through a k-*d* tree ICP variant. Papaioannou et al. [PKT01] proposed the first complete and generic computer-assisted reassembly pipeline, using GPU-accelerated distance queries. Later reassembly solutions exploited features derived from fractured regions [HFG*06], [PK03], [AMK14]. However, CH objects and bone remains frequently suffer from weathering effects, which smooth out such features. Furthermore, in other application domains, such as the automatic reassembly of mechanical parts, the involved objects can be intrinsically smooth, with no usable features. Addressing this, Thuswaldner et al. [TFK*09] combined the feature-based reassembly scheme of Huang et al. [HFG*06] with the identification of planar surfaces and straight lines. Still, this approach is limited to clean and simple forms. Zhang et al. [ZYM*15] combined the use of template objects along with a feature-based fractured region matching algorithm. Their approach is limited to thin-shell objects comprising small pieces. Wahl [WW08] proposed a featureless approach for the pairwise registration problem that maximizes contact area, using a branch-and-bound search heuristic. The authors assume reasonably large fractured surfaces, whereas their approach requires oriented point clouds. Mellado et al. [MAM14] introduced Super 4PCS, which is another example of an approach which is not based on surface features. Mavridis et al. [MAP15] employed a progressive global-to-local optimization scheme to cope with noise and outliers. Although rather general, this approach cannot be applied on heavily eroded objects where the fracture surfaces share little or no usable contact area. Andreadis et al. [APM15] used feature curves from the intact surfaces to address the matching of adjacent fragments with a minimal or even absent matching surface. Papaioannou et al. [PSA*17] proposed a shape restoration pipeline, which provides an option for using feature curves. More importantly, this work bridges object reassembly with information derived by means of shape retrieval from reference datasets.

Specialized reassembly solutions exist that tackle inherently more constrained problems, such as the reassembly of fresco pieces. Funkhouser et al. [FSTF*11] and Sizikova and Funkhouser [SF16] employed machine learning to discard incompatible combinations in frescos, whereas the method of Skembris et al. [SPK12] exploits the edge surface color texture of fresco pieces in a problem-specific fashion, which is not applicable to generic types of geometry. In their related work, Castaneda et al. [CBR*11] introduced a method for agglomerating clusters of fresco fragments by means of a global error relaxation scheme.

3. Method Overview

Fig. 1 presents the main steps of the proposed reassembly method, including fragment segmentation and facet classification, automatic feature curve extraction and mean curvature estimation, facet pair plausibility test, pairwise registration and fragment clustering leading to multi-part registration.

As a first step, each input fragment is segmented by means of region growing with a score calculated over the dihedral angles of adjacent elements, following the approach of Andreadis et al. [AMP14]. A post-processing step is required to cope with the over-segmentation resulting from region growing. For this, we employ splitting and merging of small segments, based on their average normal and normal variance. The resulting facets are classified either as fractured or intact using the local bending energy introduced by Huang et al. [HFG*06]. Considering that the local bending energy is not discriminative enough and requires adjustment of the support of the radius of the descriptor depending on the noise and local structure of the surface, we bias classification towards false positives (intact regions marked as fractured), in order to minimize the occurrence of false negatives (fractures not identified as such). This is acceptable since mistaking an intact facet for a fracture only decreases efficiency, while the opposite can lead to missing facet combinations. Finally, we merge all the intact facets for use in the following feature extraction step.

The automatic feature curve extraction step aims to identify prominent linear or curved structures of significant extent on the intact facets, which also extend towards the fractured facets and other candidate matching fragments. For this, the sphere volume integral

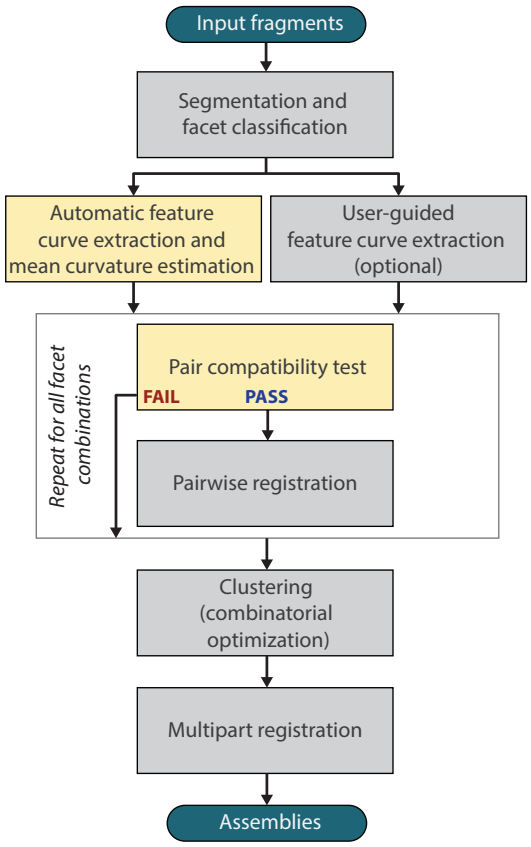

Figure 1: *The proposed reassembly pipeline. The new stages for the early combination culling are marked with yellow.*

invariant introduced by Hulin et al. [HT03] is used to derive the mean curvature at multiple scales. The points in the higher k percentage in terms of mean curvature are marked as feature points. The set of these feature points is clustered, taking into account descriptor values and spatial locations. Since we are only interested in features that span across multiple fragments, we keep features with at least one end near a fractured facet and discard the rest. Finally, each feature point cluster is approximated by the skeleton extraction method of Huang et al. [HWC*13] that uses the $L1$-median metric and does not impose specific requirements about the geometry or the topology of initial points. The feature curves are derived by approximating the resulting skeletal points by B-splines using least-squares fitting. The derived feature curves are densely sampled to generate sets of surface and extrapolated curve points, respectively. Each of these extrapolated and corresponding surface feature curves is associated with one or more of the fractured facets. As an alternative, we provide a user-guided process that extracts feature curves in a robust and efficient manner [APM15, PSA*17].

The subsequent registration steps of the pipeline are only activated for those facet pairs that pass the pair plausibility test (see next section). For fragment registration, we combine the featureless rigid geometric registration of Mavridis et al. [MAP15] for the fractured surface of the facets with the extracted feature curve point sets of the intact object's surface. The surface-based registration approach of Mavridis et al. [MAP15] is modified to include in the same minimization scheme the alignment score of the detected salient feature curves. In particular, the distance between feature curves associated with the facet under examination on one fragment and the extrapolated feature curves on the other facet and vice versa is measured and simultaneously optimized along with the corresponding contact surface. The two distinct terms, the surface metric F_{surf} and the feature curve metric F_{curve}, are defined as:

$$F_{curve} = \sum_{j=1}^{k} w_j \phi(\mathbf{M} e_j S') + \sum_{j=1}^{k'} w'_j \phi(\mathbf{M^{-1}} e'_j S') \quad (1)$$

$$F_{surf} = \sum_{i=1}^{n} \phi(\mathbf{M} x_i X') + \sum_{i=1}^{n'} \phi(\mathbf{M^{-1}} x'_i X) \quad (2)$$

where k, k' and n, n' are the number of points of E, E' and X, X' respectively. Similarly, e_j , e'_j and x_i, x'_i are the points of E, E' and X, X'. M is the rigid transformation matrix that aligns the fragments and w_j and w'_j is the exponential falloff weighting term that decreases the contribution of a measurement, the farther its location is from the valid range of the parametric curve and are combined as:

$$\arg_M min(cF_{surf} + (1-c)F_{curve}) \quad (3)$$

where c is the relative contribution of the fractured facet versus the feature curves. Weight parameter c should be set roughly proportional to the expected contact area of the two surfaces.

In case of more than two fragments, we start from the matches and respective matching errors generated in the previous stages, and compute the set of fragment clusters and corresponding global transformations of the fragment meshes. The problem is addressed by applying a variant of the graph-based approach of Huber [Hub02]. A graph is constructed, where fragments are represented as nodes and pairwise matches are the edges between nodes. The optimal set of connections is located by extraction of the Minimum Spanning Forest using the well-known Kruskal's algorithm, with the addition of penetration tests and a back-tracking scheme in order to avoid erroneous results. As a last step, iterative multipart local registration is performed in order to diffuse the propagated error due to slight shifts in the chain of applied pairwise rigid transformations.

4. Facet Pair Plausibility Test

The brute-force nature of the typical pipeline, where all possible fractured facet combinations are exhaustively considered in the registration steps, introduces a significant computational overhead. Aiming to boost reassembly efficiency, we avoid activating the registration steps in cases of implausible fractured facet pairs. For this, we introduce a heuristic approach, which compares the number of feature curves of each fractured facet, as well as the statistical properties of the geometric texture of associated intact facets. Please note that this culling step operates at a face combination level and

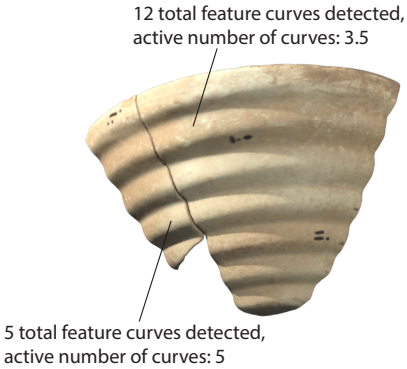

Figure 2: *Active versus actual feature curve count. during compatibility test, the number of curves compared reflect the maximum contact surface ratio of the two fragments.*

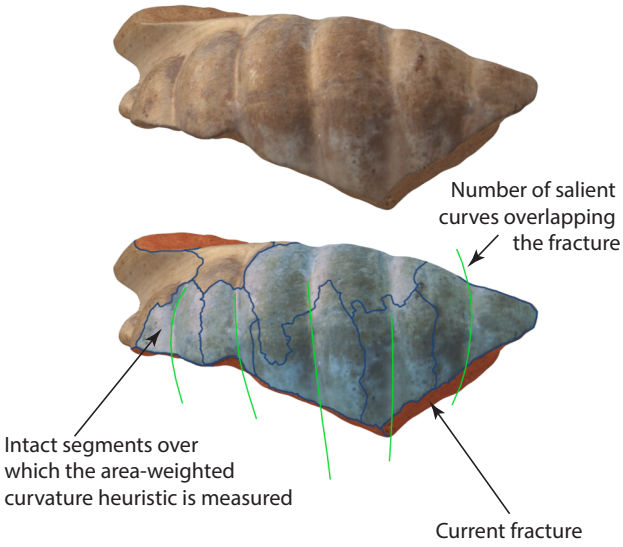

Figure 3: *The setup for the facet pair plausibility test.*

not on part combinations. Therefore, it is just as effective when only two fragments are involved. To better demonstrate this, most of the examples in the evaluation section focus on simple fragment pair matching, which clearly demonstrate the speedup, even at that granularity level.

First, only fractured facet pairs, for which the difference of the number of associated feature curves does not exceed a certain threshold t_C, is further considered. The calculation of the number of salient feature curves is based on the automatic curve extraction process explained in the previous section and re-uses this information.

To account for incompatibility issues when two fragments do not share an entire fracture surface (T-junctions), the number of feature curves for each fragment is scaled by the ratio of the opposite fragment's break surface over the maximum fracture area of both. This is illustrated in Fig. 2. In this example, the number of detected feature curves for the large and the small fragment are 12 and 5, respectively, whereas the *active* number of feature curves used is 3.5 and 5, which passes the filtering condition.

For each fractured facet pair that passes this condition, we calculate the weighted mean curvature of those intact facets that are traced by associated feature curves, weighted by the area of each intact facet:

$$\tilde{H}(i) = \sum_{j=1}^{M(i)} area(j)H(j) / \sum_{j=1}^{M(i)} area(j)) \qquad (4)$$

where $\tilde{H}(i)$ is the weighted mean curvature corresponding to fractured facet i, $M(i)$ is the number of intact facets crossed by the feature curves associated with i and $H(j)$ is the mean curvature of intact facet j. Figure 3 illustrates this computation. In this particular example, the 5 detected feature curves that are associated with the current fractured facet extend over a number of intact facets, resulting from the segmentation and classification process. We only calculate the mean curvature for those intact facets, which in the figure are highlighted with a blue colour.

All remaining pairs with a difference of $\tilde{H}$ not exceeding a second threshold t_H are selected for further evaluation. The pseudocode of this heuristic approach is presented in Algorithm 1. The standalone application of t_C will be denoted from now on as *mild filtering*, whereas the application of both thresholds, t_C and t_H, will be denoted as *full filtering*. It should be noted that the calculation of the weighted mean curvature is performed once for each fractured facet and the results are used in line 16 of function plausiblePAIRS for each facet pair. Please note (line 15) that when the number of detected curves on either of the associated intact surfaces is zero, no curvature is compared and the pair passes automatically, if the mild test is also successful.

Figure 4 illustrates examples of matching (first two columns) and incompatible (third column) pairs of fragments, in the case of no filtering, mild filtering and full filtering settings. In the first two examples, the actual, correct pair of facets is marked with a blue colour. It can be observed that the correct pair passes all filtering settings, whereas the total number of pairs passing each setting is decreasing, as expected, from no filtering to mild filtering setting.

5. Results and Evaluation

The proposed method is evaluated on real CH data that were digitized using a hand-held 3D scanner with up to 0.5 mm accuracy. All performance figures were measured on an Intel Core i7-3820 CPU at 3.6GHz.

Figure 5 shows examples of pairwise registrations with and without the use of feature curves, for the *full filtering* setting. In the case of examples 'Lion' and 'Embrasure', a usable contact surface exists allowing registration with the surface-based term of Eq. 3 (i.e. $c = 0$). In the case of examples 'Arch' and 'Embrasure', the pairs are successfully registered by co-evaluating feature curves. In the latter case, the relative contribution of the feature curves, as

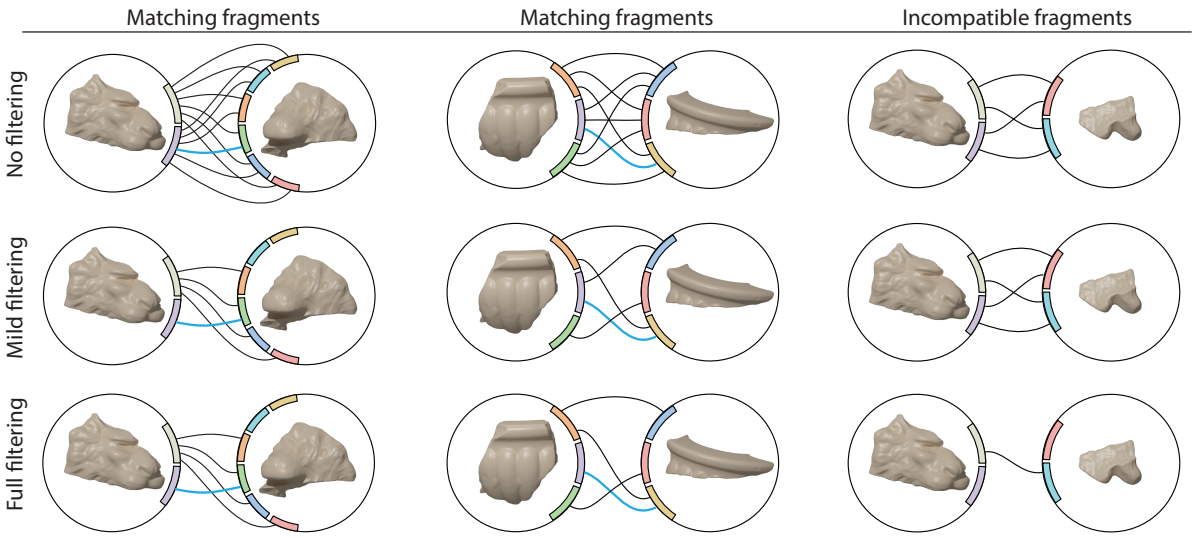

Figure 4: *Three examples of matching (first two columns) and incompatible (third column) pairs of fragments, in the case of no filtering, mild filtering and full filtering settings. The coloured slots around each fragment correspond to different facets, extracted automatically in the first step of the reassembly pipeline. In the first two examples, with blue is marked the actual, correct pair of facets.*

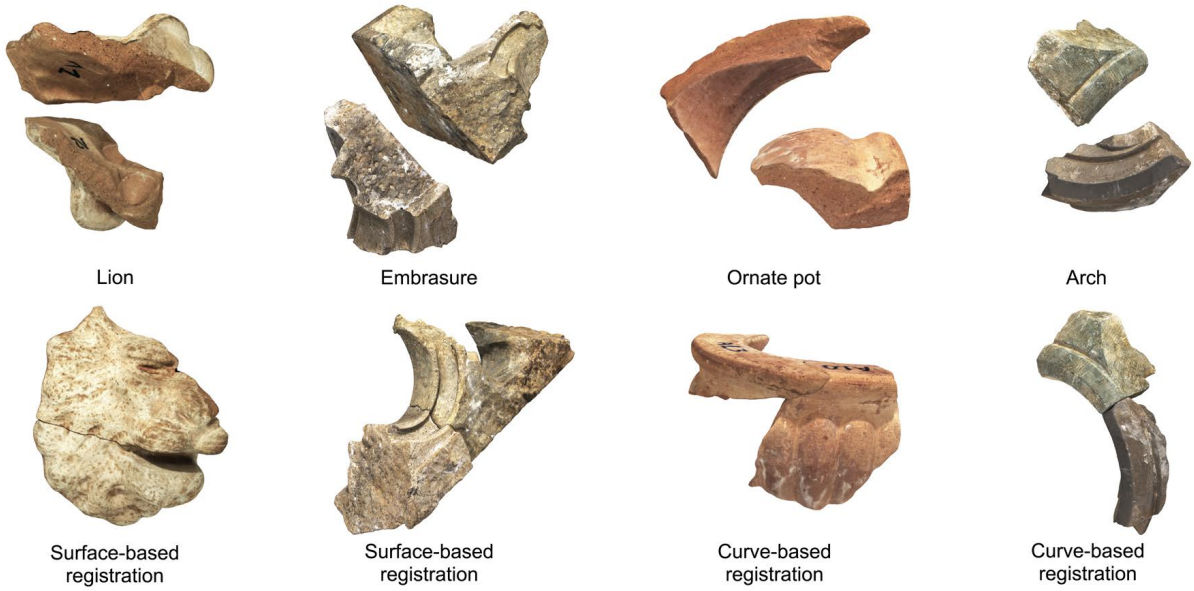

Figure 5: *The data sets used in our experiments and the corresponding reassembly results.*

quantified by c, is set to 0.85. The feature curves were derived by considering 6 scales and the lower 12.5% percentage of points detected by means of the sphere volume integral invariant of Hulin et al. [HT03]. The t_C is set to 3 and the t_H is set to 0.017. It can be observed that the proposed method successfully aligns the fragments in all examples.

Table 1 presents the number of combinations that reach the pairwise registration stage and the associated costs for three different settings: (i) the *baseline* setting, which omits the facet plausibility

Dataset	C_n	T_n **(sec)**	Speedup
Lion	12/5/5	50.2/36.7/36.4	1.3x
Embrasure	96/76/68	25.1/19.2/16.3	1.5x
Arch	30/14/10	78.9/30.1/13.4	5.8x
Ornate pot	9/5/3	37.0/19.9/15.1	2.4x

Table 1: *Number of registration tests (C_n) and total reassembly cost (T_n) in seconds with baseline/mild/full culling settings. Our method reduces up to 3 times the number of registration tests and up to 5 times the overall computation time.*

Algorithm 1 Selecting plausible pairs of facets

function PLAUSIBLEPAIRS($t_C, t_H, fragA, fragB, mode$)
  t_C: threshold in number of curves
  t_H: threshold in weighted mean curvature
  $fragA$: first fragment
  $fragB$: second fragment
  $mode$: mild/full filtering
  $segmA$: set of fractured facets of $fragA$
  $segmB$: set of fractured facets of $fragB$
  Output pairs $\mathcal{P} \leftarrow \emptyset$
  for $i \in segmA$ **do**
    for $j \in segmB$ **do**
      Nc_i: Number of associated curves on facet i
      Nc_j: Number of associated curves on facet j
      $passMild \leftarrow |Nc_i - Nc_j| < t_C$
      if mode=full AND $Nc_i \cdot Nc_j > 0$ **then**
        $passFull \leftarrow |\tilde{H}(i) - \tilde{H}(j)| < t_H$
      else
        $passFull \leftarrow true$
      if ($passMild$ AND $passFull$) **then**
        $\mathcal{P} \leftarrow \mathcal{P} \cup (i, j)$
  return $\mathcal{P}$

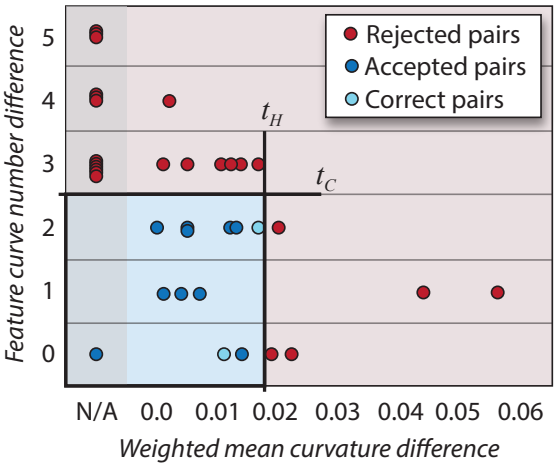

Figure 6: *Scatter plot of facet pairs in the 2D space formed by the difference in the number of associated curves Nc and the difference in weighted mean curvature $\tilde{H}$.*

test described in subsection 4, (ii) the *mild filtering* setting, which only compares the number of feature curves, (iii) the *full filtering* setting, which employs the full facet plausibility test. It can be observed that the number of combinations tested with accurate pairwise registration is consistently decreasing, from the *baseline* to the *mild filtering* and the *full filtering* setting. Moreover, the computational cost of registration is significantly reduced, more than 5 times in the case of the *Arch* data set.

Figure 6 presents a scatter plot in the parametric space of the difference in the number of associated curves Nc and the difference in weighted mean curvature $\tilde{H}$ for the facet pairs in Figure 5. Each sample in the scatter plot corresponds to a tested facet combination

Figure 7: *Reassembly of three fragments of the 'Lion' object, using surface-based registration.*

from both matching and incompatible fragments. The value 'N/A' in the horizontal axis indicates facet pairs from which at least one facet has no associated feature curve and therefore, the difference in weighted mean curvature cannot be defined. Still, several facet pairs of this case are filtered out. As can be observed, the majority of the non-matching pairs are rejected due to the feature curve difference criterion ('mild' filtering with threshold t_C). The curvature-based combination culling is good at isolating cases, where the relief of the intact surface of the two fragments is distinctly different (see values in the 0.04-0.06 range), either corresponding to significantly disjoint areas of the object to be reassembled or to different objects.

All the examples of Fig. 5 and Fig. 6 presented the registration of a pair of fragments. As described in Section 3, the proposed approach can be applied for the reassembly of more than two fragments. Figure 7 presents the results for three fragments, when applying the 'full filtering' settings. It can be observed that once more, the proposed method successfully assembles the three fragments. Moreover, instead of exhaustively examining 116 facet combinations, the proposed approach examines only 69 combinations. Figure 8 shows a case of a combination that due to trivial surface compatibility, the matching error of the surface-based registration promoted the particular combination as the best candidate, in the baseline case (no filtering). When the combination filtering was enabled, the erroneous combination was culled, resulting in a correct optimal pairing, shown in Figure 5.

6. Conclusions and Future Work

This work presents an efficient approach for pruning fragment combinations in general 3D pairwise registration tasks during computational reassembly of CH artefacts. The method prevents inherently incompatible fragment sides from being considered for geometric matching and registration by examining the geometric compatibility of the intact areas of each pair part near the fracture, since the fractured area itself may or may not be a reliable source of infor-

Figure 8: *Suboptimal solution reached by* baseline *setting for 'Dora embrasure', which has been filtered-out by mild filtering and full filtering settings. The optimal solution is illustrated in Fig. 5.*

mation due to erosion or mechanical damage. Our experiments on scanned real fragments indicate that the facet pair plausibility test significantly reduces the computational cost, while the proposed approach remains effective, even in cases where contact area is unusable.

It is important to note that any pruning strategy can potentially introduce false negatives, i.e. may cull important matches and the proposed approach is no different; the validity of the results depends on how aggressive the filtering thresholds t_C and t_H are. Although throughout our experiments the settings did not vary, despite the differences in material and scale of the fragments tested, it is highly probable that for larger datasets with significant variation in fractured surface area, a more conservative parameterization should be preferred. Experimentation on large-scale datasets to evaluate the robustness against threshold settings is a priority for our future work. We would like to also consider textural patterns near the fracture lines, keeping in mind though that such a filtering approach is only applicable to well-preserved man-made colourings and not the base material texture, since the weathering conditions for each fragment may vastly differ.

Acknowledgements

The research leading to these results has received funding from the European Union's Seventh Framework Programme (FP7/2007-2013) under Grant agreement no. 600533 PRESIOUS.

References

[AMK14] ALTANTSETSEG E., MATSUYAMA K., KONNO K.: Pairwise matching of 3D fragments using fast Fourier transform. *Vis. Comput. 30*, 6-8 (2014), 929–938. 2

[AMP14] ANDREADIS A., MAVRIDIS P., PAPAIOANNOU G.: Facet extraction and classification for the reassembly of fractured 3d objects. In *Proc. Eurographics (poster)* (2014), pp. 1–2. 2

[APM15] ANDREADIS A., PAPAIOANNOU G., MAVRIDIS P.: Generalized digital reassembly using geometric registration. In *Proc. Digital Heritage* (2015), pp. 549–556. 2, 3

[CBR*11] CASTAÑEDA A. G., BROWN B., RUSINKIEWICZ S., FUNKHOUSER T., WEYRICH T.: Global consistency in the automatic assembly of fragmented artefacts. In *Proc. Int. Symposium on Virtual Reality, Archaeology and Cultural Heritage (VAST)* (2011). 2

[DD07] DEMAINE E. D., DEMAINE M. L.: Jigsaw puzzles, edge matching, and polyomino packing: Connections and complexity. *Graphs and Combinatorics 23*, 1 (2007), 195–208. 1, 2

[FSTF*11] FUNKHOUSER T., SHIN H., TOLER-FRANKLIN C., CASTAÑEDA A. G., BROWN B., DOBKIN D., RUSINKIEWICZ S., WEYRICH T.: Learning how to match fresco fragments. *J. Comput. Cultural Heritage 4*, 2 (2011), 7:1–7:13. 1, 2

[HFG*06] HUANG Q.-X., FLÖRY S., GELFAND N., HOFER M., POTTMANN H.: Reassembling fractured objects by geometric matching. In *Proc. ACM SIGGRAPH* (2006), pp. 569–578. 2

[HT03] HULIN D., TROYANOV M.: Mean curvature and asymptotic volume of small balls. *The American Mathematical Monthly 110*, 10 (2003), 947–950. 3, 5

[Hub02] HUBER D.: *Automatic three-dimensional modeling from Reality*. PhD thesis, Carnegie Mellon University, 2002. 3

[HWC*13] HUANG H., WU S., COHEN-OR D., GONG M., ZHANG H., LI G., CHEN B.: L_1-medial skeleton of point cloud. *ACM Trans. Graph. 32*, 4 (2013), 65:1–65:8. 3

[MAM14] MELLADO N., AIGER D., MITRA N. J.: Super 4PCS fast global pointcloud registration via smart indexing. *Comput. Graph. Forum 33*, 5 (2014), 205–215. 2

[MAP15] MAVRIDIS P., ANDREADIS A., PAPAIOANNOU G.: Fractured object reassembly via robust surface registration. In *Proc. Eurographics (short paper)* (2015), pp. 21–24. 2, 3

[MRS10] MELLADO N., REUTER P., SCHLICK C.: Semi-automatic geometry-driven reassembly of fractured archeological objects. In *Proc. Intl. Symposium on Virtual Reality, Archaeology and Cultural Heritage (VAST)* (2010), pp. 33–38. 2

[PK03] PAPAIOANNOU G., KARABASSI E.: On the automatic assemblage of arbitrary broken solid artefacts. *Image Vision Comput. 21*, 5 (2003), 401–412. 1, 2

[PKT01] PAPAIOANNOU G., KARABASSI E.-A., THEOHARIS T.: Virtual archaeologist: assembling the past. *IEEE Computer Graphics and Applications 21* (2001), 53–59. 2

[PSA*17] PAPAIOANNOU G., SCHRECK T., ANDREADIS A., MAVRIDIS P., GREGOR R., SIPIRAN I., VARDIS K.: From reassembly to object completion: A complete systems pipeline. *J. Comput. Cultural Heritage 10*, 2 (2017), 8:1–8:22. 2, 3

[SF16] SIZIKOVA E., FUNKHOUSER T.: Wall painting reconstruction using a genetic algorithm. In *Proc. Eurographics Workshop on Graphics and Cultural Heritage (GCH)* (2016). 1, 2

[SPK12] SKEMBRIS A. S., PAPAODYSSEUS C., KOUKOUTSIS E.: 2D fragmented object reconstruction with the use of the chromatic and thematic content. *Pattern Anal. Appl. 15*, 2 (2012), 133–146. 2

[SRE*01] SCHEUERING M., REZK-SALAMA C., ECKSTEIN C., HORMANN K., GREINER G.: Interactive repositioning of bone fracture segments. In *Proc. Vision Modeling and Visualization* (2001), pp. 499–506. 2

[TFK*09] THUSWALDNER B., FLÖRY S., KALASEK R., HOFER M., HUANG Q.-X., THÜR H.: Digital anastylosis of the octagon in ephesos. *J. Comput. Cultural Heritage 2*, 1 (2009), 1–27. 2

[WAT*07] WILLIS A., ANDERSON D., THOMAS T., BROWN T., MARSH J. L.: 3D reconstruction of highly fragmented bone fractures. In *Proc. SPIE* (2007), vol. 6512. 2

[WW08] WINKELBACH S., WAHL F. M.: Pairwise matching of 3D fragments using cluster trees. *Int. J. of Computer Vision 78*, 1 (2008), 1–13. 2

[ZWS*09] ZHOU B., WILLIS A., SUI Y., ANDERSON D. D., BROWN T. D., THOMAS T. P.: Virtual 3D bone fracture reconstruction via inter-fragmentary surface alignment. In *Proc. Int. Conference on Computer Vision Workshops* (2009), pp. 1809–1816. 2

[ZYM*15] ZHANG K., YU W., MANHEIN M., WAGGENSPACK W. N., LI X.: 3D fragment reassembly using integrated template guidance and fracture-region matching. In *Proc. Int. Conference on Computer Vision* (2015), pp. 2138–2146. 2